J Mater Sci: Mater Med (2011) 22:601–606
DOI 10.1007/s10856-010-4227-x

Magnetic resonance imaging probes for labeling of chondrocyte cells

Gang Liu · Chunchao Xia · Zhiyong Wang · Fei Lv · Fabao Gao · Qiyong Gong · Bin Song · Hua Ai · Zhongwei Gu

Received: 24 June 2010 / Accepted: 23 December 2010 / Published online: 30 January 2011

Abstract Recent progress in cell therapy research has raised the need for non-invasive monitoring of transplanted cells. Magnetic resonance imaging (MRI) of superparamagnetic iron oxide (SPIO) labeled cells have been widely used for high resolution monitoring of the biodistribution of cells after transplantation. Here we report that self-assembly of amphiphilic polyethylenimine (PEI)/SPIO nanocomposites can lead to the formation of ultrasensitive MRI probes, which can be used to label chondrocyte cells with good biocompatibility. The labeled cells display strong signal contrast compared to unlabeled ones in a clinical MRI scanner. This probe may be useful for non-invasive MR tracking of implanted cells for tissue regeneration.

Gang Liu and Chunchao Xia contributed equally to this work.

G. Liu · Z. Wang · F. Lv · H. Ai (✉) · Z. Gu
National Engineering Research Center for Biomaterials, Sichuan University, Chengdu 610064, China
e-mail: huaai@scu.edu.cn

C. Xia · F. Gao · Q. Gong · B. Song · H. Ai
Department of Radiology, West China Hospital, Sichuan University, Chengdu 610041, China

G. Liu
Institute of Materia Medica and Department of Pharmacology, North Sichuan Medical College, Nanchong, Sichuan 637007, China

G. Liu
Sichuan Key Laboratory of Medical Imaging, Department of Radiology, North Sichuan Medical College, Nanchong 637007, China

1 Introduction

Cell transplantation not only has the ability to provide therapeutic agents, it also has the potential to repair and replace tissue lost to injury/disease [1–4]. Successful application of cell-based approaches in clinical therapies requires techniques to monitor engrafted cell survival and integration non-invasively and dynamically with a high temporal and spatial resolution [5, 6]. Conventional histological methods, however, suffer from substantial drawbacks and do not allow longitudinal studies of transplanted cells. With recent developments, magnetic resonance imaging (MRI) provides high spatial resolutions [5, 7–9] and various cell labeling approaches based on superparamagnetic iron oxide (SPIO) have been used to visualize cell migration and distribution by MRI [10–15].

Generally, most SPIO nanoparticles are covered with dextran or poly(ethylene glycol) (PEG) for improved biocompatibility, reduced non-specific protein binding, and prolonged circulation in biological systems [16]. However, the SPIO nanoparticles coated with dextran or PEG have limitation to label cells because the negative or non-charge surface reduces the non-specific particle uptake [17]. To facilitate SPIO labeling of cells, much effort has been directed toward developing suitable procedures for efficient intracellular labeling, such as complexing of polycationic transfection agents to SPIO [18–22]. In our previous work, we have designed and developed novel SPIO nanocomposites using amphiphilic *N*-dodecyl-polyethylenimine (PEI) [23]. This nanocomposite system has great potential to label biological cells for cellular transplantation research.

The aim of this study was to develop a simple protocol to label chondrocyte cells using low molecular weight amphiphilic PEI/SPIO nanocomposites at optimized low dosages. Our data showed amphiphilic PEI/SPIO

nanocomposites could be used to label chondrocyte cells with high efficiency. The SPIO-labeling process was found not to affect the viability of the chondrocyte cells or the production of major cartilage matrix constituents. This probe provides us opportunities to track chondrocyte cells under MRI during cell-based therapies for cartilage regeneration.

2 Materials and methods

2.1 Synthesis of SPIO nanocomposites

SPIO nanoparticles were synthesized using Iron (III) acetylacetonate as precursors in benzyl ether at high temperatures [23]. The as-synthesized particles were purified through ethanol wash and stored in hexane. Amphiphilic polyethylenimine (PEI) was synthesized through alkylation of branched PEI-2k with 1-iododododecane. SPIO nanoparticles were transferred into aqueous phase with the help of amphiphilic PEI following a previous method [23]. The size and charge of nanocomposites were characterized by dynamic light scattering (DLS) and zeta-potential measurement. The overall morphology of nanocomposites was investigated under transmission electron microscope (TEM) as previously described [24]. The T_2 (transverse) relaxivity and detection limit of this probe was measured at room temperature in a clinical 3T MRI scanner similar to our previous work [25].

2.2 Rabbit chondrocyte cell culture and labeling

Chondrocyte cells were isolated by sequential enzymatic digestion from the articular cartilage of joints of newborn New Zealand white rabbits [26]. After digestion, isolated chondrocyte cells were filtered to remove any undigested cartilage particles and washed three times with PBS, and cells were resuspended in α-MEM supplemented with 1% ascorbic acid, 10% fetal bovine serum and 1% penicillin–streptomycin. When the cells of the first passage reached 80–90% confluence, they were labeled with amphiphilic PEI/SPIO nanocomposites for 24 h at an iron concentration of 5 μg/ml. The imaging probe labeling efficiency was evaluated by Prussian blue staining.

2.3 Cell viability

For assessment of toxicity of the imaging probe labeling on chondrocyte cells, cells were evaluated by using 3-(4,5-dimethylthiazol-2-yl)-2,5-diphenyl tetrazolium bromide (MTT) assays [27]. The chondrocyte cells after treatment with nanoparticles for 24 h were allowed to grow in regular growth medium for 24 h followed by incubation with MTT reagent. The dark blue formazan dye generated by the live cells was proportional to the number of live cells and the absorbance at 570 nm was measured. For apoptosis studies, the labeled and untreated cells were incubated with Hoechst 33258 for 10 min at room temperature. Cells showing condensed chromatin were determined as apoptotic [27]. The percentage of apoptotic cells was counted and averaged over five fields of microscopic observation in each sample (80–100 cells each field).

2.4 Western blot analysis

The expression of ferritin was semiquantitatively detected using western blotting technique. After 24 h of labeling, the chondrocytes were washed with phosphate buffer three times and centrifuged at 1000 rpm for 5 min to form cell pellets. Modified RIPA buffer was added into resuspend and lyse cell pellets at 4°C for 30 min.Then the lysates were centrifuged at 12000 rpm for 15 min and supernatants were collected. BCA Protein Assay (Pierce Biotechnology) was used to measure protein concentration according to the manufacturer's instructions. Total amount of 30 μg protein was loaded per well and subjected to sodium dodecyl sulfate polyacrylamide gel electrophoresis (SDS-PAGE) on 12% gels. After electrophoresis, proteins were transferred onto 0.4 μm PVDF (Millipore) membranes and ferritin heavy chain expression was detected using goat polyclonal antibody (Santa Cruz Biotechnology) at a dilution of 1:200. Then immunocomplexes were detected by horseradish peroxidase (HRP)-conjugated (1:2000) secondary antibodies. Protein bands were visualized by ECL kit (Pierce Biotechnology) and the images were captured using FluorChem™ (Alpha Innotech). Relative amount of immune complexes were estimated by Image J software (Broken Symmetry) and normalized to β-actin.

2.5 Biochemical assays

For glycosaminoglycan (GAG) assays, the labeled chondrocytes were cultured in serum-free medium containing insulin-transferrin-selenious acid mix medium supplemented with 100 nM dexamethasone and 10 ng/ml transforming growth factor-β and the culture ended after 21 days, at which time cells were stained with Safranin O and toluidine blue, respectively [15]. For collagen type II detection, immunohistochemical staining was performed according to the instructions of the manufacturer (Santa Cruz Biotechnology). Expressions of collagen type II was observed under an inverted phase contrast microscope and percentage of positive cells in each sample was counted.

2.6 Cellular MRI

The labeled cells were trypsinized and counted using a hemocytometer. After centrifugation, the labeled cells were then embedded into collagen type I hydrogel and examined with a clinical 3T MRI scanner to investigate the imaging efficacy. In brief, labeled cells were embedded in collagen type I hydrogel (serial dilutions of cells were prepared in 0.2 ml collagen hydrogels with a final cell number of 2×10^6, 10^6, 2×10^5, 10^5, and 5×10^4) at a collagen concentration of 3 mg/ml. The collagen-cell suspension was pipetted into 96-well culture plates and the collagen hydrogels were cultivated to allow air bubbles to disappear before MR imaging. MRI study of these collagen hydrogels was performed at 3 Tesla (GE Signa Excite) using a clinical knee coil. T_2 spin echo scans were used with the following parameters: TR = 5000 ms, TE from 10 to 500 ms, number of averages = 1, matrix = 384 × 224, FOV = 250 × 190 mm, slice thickness = 2.0 mm. Signal intensities of different TE time were used to calculate the T_2 value of each cell sample.

2.7 Statistical analysis

Data were expressed as mean ± SD (n = 3). Statistical analysis was performed using Student's t test and Chi-square test. $P < 0.05$ was considered statistically significant.

3 Results and discussion

3.1 Amphiphilic PEI/SPIO nanocomposites and cell labeling

Cellular MRI has enabled high-resolution, noninvasive, and serial imaging of labeled cells migration into damaged tissues for studying of repairing, replacement, or therapy strategies in diseases [28–30]. SPIO nanoparticles are emerging as ideal probes for noninvasive cell tracking. However, the cellular labeling efficiency of probes depends on a number of factors, including cell type, size and surface properties of SPIO nanoparticles [17, 31, 32].

In our study, hydrophobic SPIO nanoparticles could be transferred from organic solvent into water with the help of amphiphilic PEI. DLS and TEM analysis showed that most nanocomposites were about 60–70 nm (peak) in diameter without obvious aggregation (Fig. 1). The SPIO nanocomposites were strongly positively charged with zeta-potentials in the range of 50–65 mV, which is helpful for their binding to cell membrane for subsequent uptake. At the magnetic field of 3T, the T_2 relaxivity of the PEI/SPIO

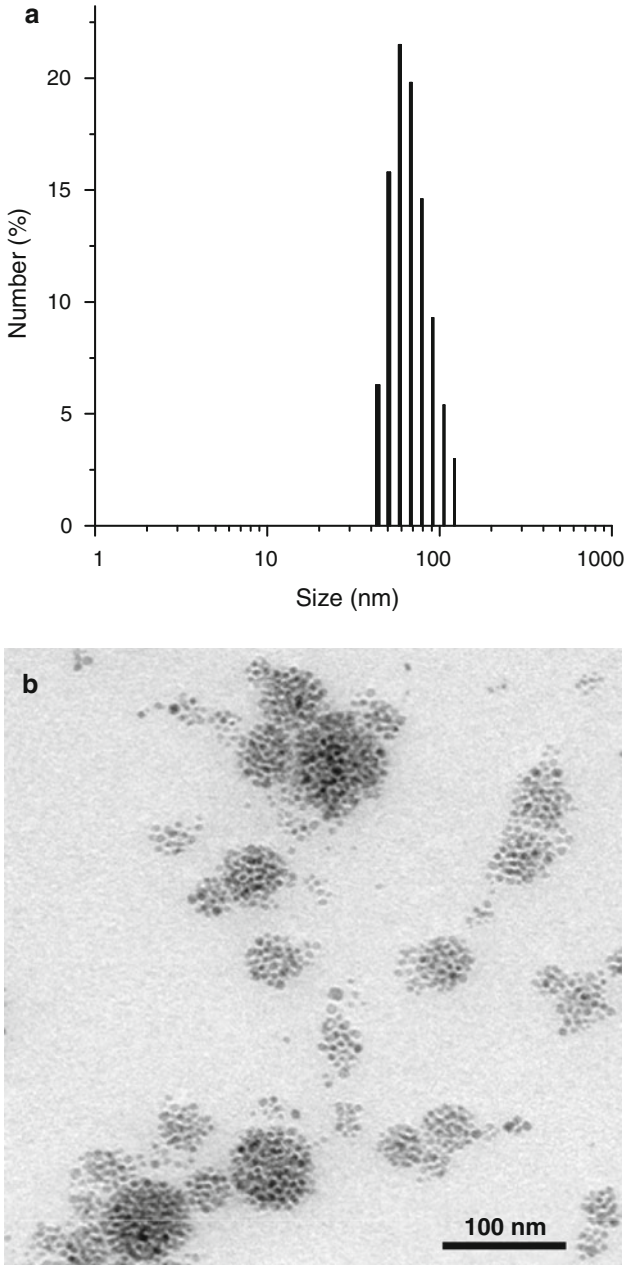

Fig. 1 DLS and TEM analysis of amphiphilic PEI/SPIO nanocomposites

nanocompoaite was 389 Fe mM^{-1} s^{-1} and the detection limit (spin-echo sequence: TR = 5000 ms, TE = 55 ms) is about 2 μg/ml Fe. Chondrocyte cells could be directly labeled with the high quality probe by adding nanocomposites to the culture medium, and nearly 100% of the chondrocytes were labeled after 24 h incubation with SPIO at the low iron concentration (5 μg/ml), as evidenced by Prussian blue staining (data not shown). This labeling procedure is straightforward as it does not require any additional transfection agent.

3.2 The biocompatibility of amphiphilic PEI/SPIO nanocomposites

For cell tracking, the biological effects of the internalized nanoparticles should be carefully investigated [27]. Specifically, for chondrocyte cells, it is important to determine whether any detrimental effects on cell proliferation, cellular iron homeostasis and immunomodulatory property following labeling, all of which are critical factors involved in the regenerative and therapeutic potentials of chondrocyte cells [13, 33, 34].

To evaluate any possible cytotoxic effects of amphiphilic PEI/SPIO nanocomposites, cell viability was examined. After labeling using the amphiphilic PEI/SPIO nanocomposites, the morphology of these labeled chondrocytes was similar to unlabeled ones. Results of MTT assay showed that labeled cells have similar proliferation comparing to those untreated cells (Fig. 2).

Edyta Pawelczyk et al. [35] analyzed ferritin expression of Hela, primary macrophage and MSCs after labeling with Ferumoxide-protamine sulfate complexes, their results demonstrated these three kinds of cells increased ferritin expression in response to ferumoxide loading into endosomes. In our experiment of western blot analysis,

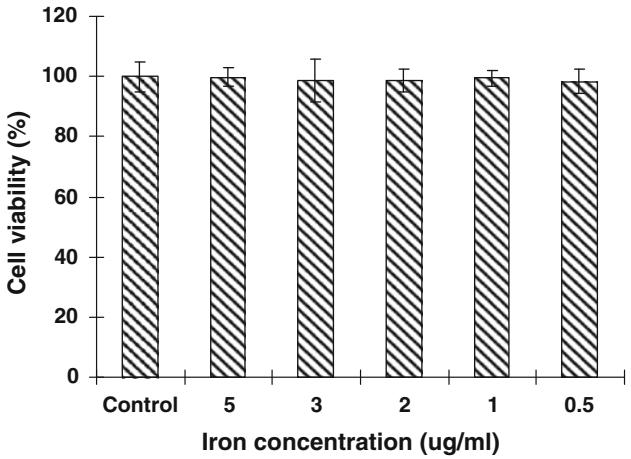

Fig. 2 Cytotoxicities of the amphiphilic PEI/SPIO nanocomposites were evaluated 48 h after labeling for 4 h using the MTT assay

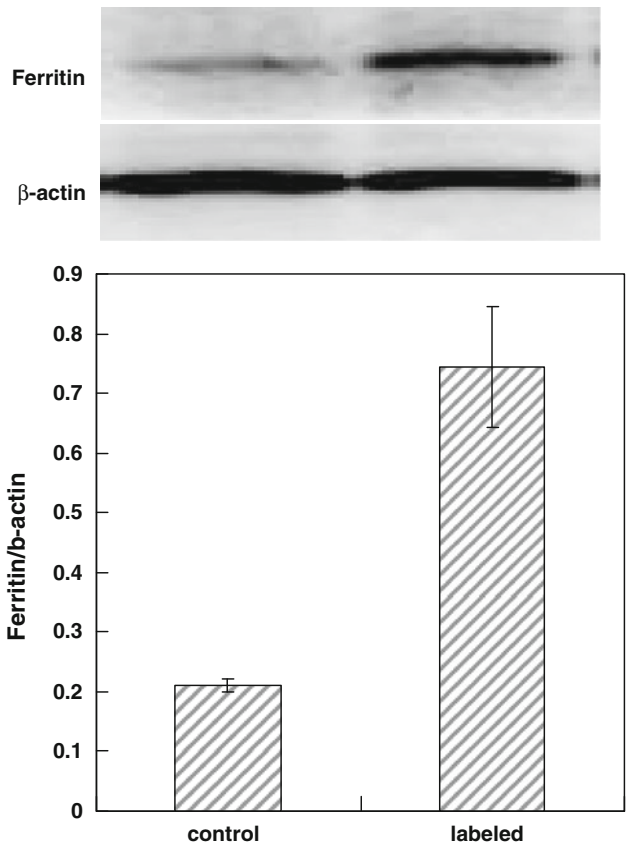

Fig. 3 Ferritin protein expression was up-regulated in SPIO probe labeled chondrocyte cells. *Lower panel*: ratios of protein quantification of ferritin to β-actin

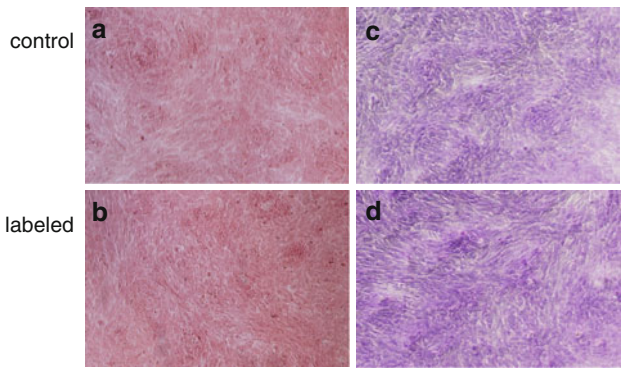

Fig. 4 Safranin O (**a**, **b**) and toluidine blue (**c**, **d**) assay of unlabeled (**a**, **c**) and labeled (**b**, **d**) chondrocyte cells. No statistical significance in the formation and accumulation of cartilage matrix constituents (GAG) between labeled and non-labeled chondrocyte cells

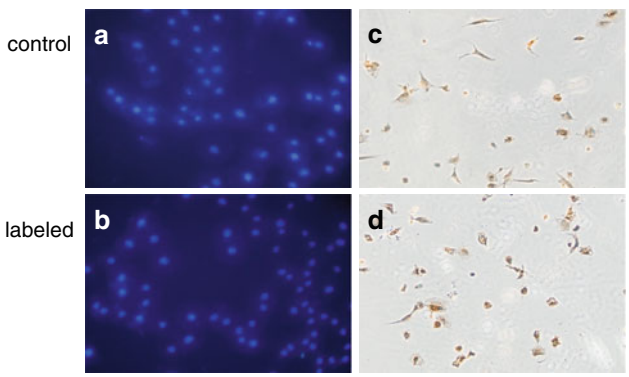

Fig. 5 Hoechst (**a, b**) and immunohistochemical staining (**c, d**) of unlabeled (**a**, **c**) and labeled (**b**, **d**) chondrocyte cells. There was no obvious difference in apoptosis and collagen type II protein expression between labeled and unlabeled chondrocyte cells

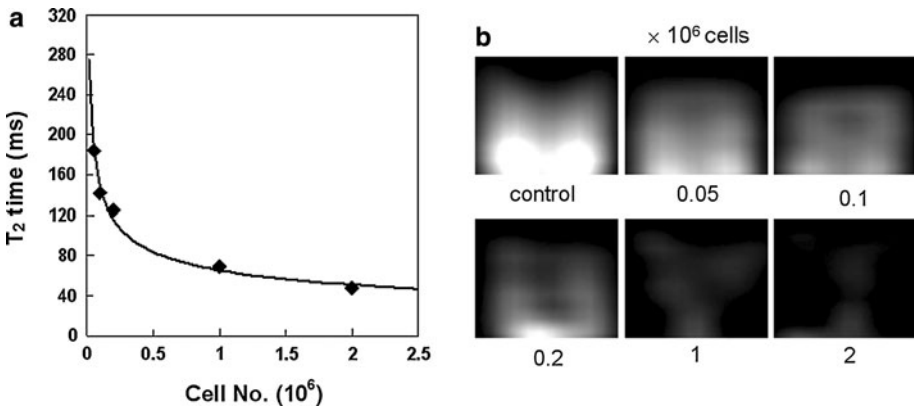

Fig. 6 Magnetic resonance images of amphiphilic PEI/SPIO nanocomposites labeled chondrolyte cells. **a** T_2 values of labeled cells as a function of cell number at 3T; **b** MRI images of labeled and unlabeled cells in collagen matrix

chondrocytes also obviously elevated the ferritin expression after the SPIO nanoparticles incorporated into the cells. It is well known that ferritin synthesis can be induced with an increase in cytoplasmic iron content, resulting in sequestration of toxic iron into the ferritin molecules [36]. Since it is possible that labeled chondrocyte cells may contain SPIO nanoparticles for long periods of time, it is necessary to determine if the iron can be released from the endosome/lysosome compartment and become available to the metabolic pathways. Up-regulation of ferritin in labeled cells (Fig. 3) provides evidence that excess iron can be stored in ferritins, thus protecting the cells from possible cytotoxicity led by higher intracellular iron concentrations.

As shown in Fig. 4, the formation and accumulation of cartilage matrix constituents (GAG) could be observed after 21-day incubation in cells cultured in chondrogenic medium regardless of treatment with nanoparticles or not. Besides, there was no obvious difference in Safranin O and toluidine blue stain assay between amphiphilic PEI/SPIO nanocomposites treated and untreated cells. In addition, immunocytochemistry assay showed the collagen type II protein expression of the labeled cells was unchanged (Fig. 5). Apoptosis assay showed that less than 5% of the labeled chondrocyte cells were apoptotic, as the same as the unlabeled cells (Fig. 5). Taken together, this imaging probe has good biocompatibility for chondrocyte cells labeling without affecting their major functions.

3.3 MRI study of labeled cells

Magnetic resonance images of SPIO labeled cells in tissues on T_2 or T_2-weighted images are hypointense regions associated with a blooming susceptibility artifact resulting from the clustering of SPIO within endosomes in cells. To check the sensitivity of the probe labeling and to estimate signal behavior in vivo, labeled cells were embedded in collagen type I hydrogels and we performed in vitro imaging of the three-dimensional matrix. Cellular MRI showed that T_2 values decrease with the increase of cell number (5×10^4–2×10^6) from 184 to 48 ms, which can provide noticeable signal contrast comparing to unlabeled cells (Fig. 6). This method of visualizing chondrocyte cells may be useful in further development of tissue engineered cartilage therapeutics, because it can be used in longitudinal tracking of chondrocyte cells in vivo and provide more important information.

4 Conclusions

In summary, self-assembly of amphiphilic PEI/SPIO nanocomposites led to the formation of ultrasensitive MRI probes, which can be used to label chondrocyte cells with good biocompatibility. The labeled cells display strong signal contrast to unlabeled cells in a clinical MRI scanner. This probe may be useful for noninvasive MR tracking of implanted cells for tissue regeneration.

Acknowledgment The work was supported by Program for New Century Excellent Talents in University (NCET-06-0781), Distinguished Young Scholars Project of Sichuan Province (06ZQ026-007), and National Natural Science Foundation of China (20974065, 50603015, and 50830107).

References

1. Kurozumi K, Nakamura K, Tamiya T, Kawano Y, Ishii K, Kobune M, Hirai S, Uchida H, Sasaki K, Ito Y, Kato K, Honmou O, Houkin K, Date I, Hamada H. Mesenchymal stem cells that produce neurotrophic factors reduce ischemic damage in the rat middle cerebral artery occlusion model. Mol Ther. 2005;11:96–104.
2. Satake K, Lou J, Lenke LG. Migration of mesenchymal stem cells through cerebrospinal fluid into injured spinal cord tissue. Spine (Phila Pa 1976). 2004;29:1971–9.
3. Trippel SB. Autologous chondrocyte transplantation. N Engl J Med. 1995;332:539–40.
4. van Osch GJ, Brittberg M, Dennis JE, Bastiaansen-Jenniskens YM, Erben RG, Konttinen YT, Luyten FP. Cartilage repair: past and future–lessons for regenerative medicine. J Cell Mol Med. 2009;13:792–810.

5. Weissleder R, Mahmood U. Molecular imaging. Radiology. 2001;219:316–33.
6. Schroeder T. Imaging stem-cell-driven regeneration in mammals. Nature. 2008;453:345–51.
7. Smith BR, Johnson GA, Groman EV, Linney E. Magnetic resonance microscopy of mouse embryos. Proc Natl Acad Sci USA. 1994;91:3530–3.
8. Bulte JW, Kraitchman DL. Iron oxide MR contrast agents for molecular and cellular imaging. NMR Biomed. 2004;17:484–99.
9. Jacobs RE, Fraser SE. Magnetic resonance microscopy of embryonic cell lineages and movements. Science. 1994;263: 681–4.
10. Frank JA, Zywicke H, Jordan EK, Mitchell J, Lewis BK, Miller B, Bryant LH Jr, Bulte, JW. Magnetic intracellular labeling of mammalian cells by combining (FDA-approved) superparamagnetic iron oxide MR contrast agents and commonly used transfection agents. Acad Radiol. 2002; 9 Suppl 2:S484–7.
11. Lu CW, Hung Y, Hsiao JK, Yao M, Chung TH, Lin YS, Wu SH, Hsu SC, Liu HM, Mou CY, Yang CS, Huang DM, Chen YC. Bifunctional magnetic silica nanoparticles for highly efficient human stem cell labeling. Nano Lett. 2007;7:149–54.
12. Smirnov P, Lavergne E, Gazeau F, Lewin M, Boissonnas A, Doan BT, Gillet B, Combadiere C, Combadiere B, Clement O. In vivo cellular imaging of lymphocyte trafficking by MRI: a tumor model approach to cell-based anticancer therapy. Magn Reson Med 2006;56:498–508.
13. Ramaswamy S, Greco JB, Uluer MC, Zhang Z, Fishbein KW, Spencer RG. Magnetic resonance imaging of chondrocytes labeled with superparamagnetic iron oxide nanoparticles in tissue-engineered cartilage. Tissue Eng Part A. 2009;15:3899–910.
14. Li Z, Suzuki Y, Huang M, Cao F, Xie X, Connolly AJ, Yang PC, Wu JC. Comparison of reporter gene and iron particle labeling for tracking fate of human embryonic stem cells and differentiated endothelial cells in living subjects. Stem Cells. 2008;26:864–73.
15. Heymer A, Haddad D, Weber M, Gbureck U, Jakob PM, Eulert J, Noth U. Iron oxide labelling of human mesenchymal stem cells in collagen hydrogels for articular cartilage repair. Biomaterials. 2008;29:1473–83.
16. Sun S. Recent advances in chemical synthesis, self-assembly, and applications of FePt nanoparticles. Adv Mater. 2006;18:393–403.
17. Metz S, Bonaterra G, Rudelius M, Settles M, Rummeny EJ, Daldrup-Link HE. Capacity of human monocytes to phagocytose approved iron oxide MR contrast agents in vitro. Eur Radiol. 2004;14:1851–8.
18. Ahrens ET, Feili-Hariri M, Xu H, Genove G, Morel PA. Receptor-mediated endocytosis of iron-oxide particles provides efficient labeling of dendritic cells for in vivo MR imaging. Magn Reson Med. 2003;49:1006–13.
19. Arbab AS, Yocum GT, Kalish H, Jordan EK, Anderson SA, Khakoo AY, Read EJ, Frank JA. Efficient magnetic cell labeling with protamine sulfate complexed to ferumoxides for cellular MRI. Blood. 2004;104:1217–23.
20. Babic M, Horak D, Trchova M, Jendelova P, Glogarova K, Lesny P, Herynek V, Hajek M, Sykova E. Poly(L-lysine)-modified iron oxide nanoparticles for stem cell labeling. Bioconjug Chem. 2008;19:740–50.
21. Yeh TC, Zhang W, Ildstad ST, Ho C. In vivo dynamic MRI tracking of rat T-cells labeled with superparamagnetic iron-oxide particles. Magn Reson Med. 1995;33:200–8.
22. Zhang C, Jugold M, Woenne EC, Lammers T, Morgenstern B, Mueller MM, Zentgraf H, Bock M, Eisenhut M, Semmler W, Kiessling F. Specific targeting of tumor angiogenesis by RGD-conjugated ultrasmall superparamagnetic iron oxide particles using a clinical 1.5-T magnetic resonance scanner. Cancer Res. 2007;67:1555–62.
23. Wang Z, Liu G, Sun J, Wu B, Gong Q, Song B, Ai H, Gu Z. Self-assembly of magnetite nanocrystals with amphiphilic polyethylenimine: structures and applications in magnetic resonance imaging. J Nanosci Nanotechnol. 2009;9:378–85.
24. Lu J, Ma S, Sun J, Xia C, Liu C, Wang Z, Zhao X, Gao F, Gong Q, Song B, Shuai X, Ai H, Gu Z. Manganese ferrite nanoparticle micellar nanocomposites as MRI contrast agent for liver imaging. Biomaterials. 2009;30:2919–28.
25. Ai H, Flask C, Weinberg B, Shuai X, Pagel M, Farrell D, Duerk J, Gao J. Magnetite-loaded polymeric micelles as ultrasensitive magnetic resonance probes. Adv Mater. 2005;17:1949–52.
26. Zheng L, Sun J, Chen X, Wang G, Jiang B, Fan H, Zhang X. In vivo cartilage engineering with collagen hydrogel and allogenous chondrocytes after diffusion chamber implantation in immunocompetent host. Tissue Eng Part A. 2009;15:2145–53.
27. Liu G, Tian J, Liu C, Ai H, Gu Z, Gou J, Mo X. Cell labeling efficiency of layer-by-layer self-assembly modified silica nanoparticles. J Mater Res. 2009;24:1317–21.
28. Anderson SA, Glod J, Arbab AS, Noel M, Ashari P, Fine HA, Frank JA. Noninvasive MR imaging of magnetically labeled stem cells to directly identify neovasculature in a glioma model. Blood. 2005;105:420–5.
29. Hill JM, Dick AJ, Raman VK, Thompson RB, Yu ZX, Hinds KA, Pessanha BS, Guttman MA, Varney TR, Martin BJ, Dunbar CE, McVeigh ER, Lederman RJ. Serial cardiac magnetic resonance imaging of injected mesenchymal stem cells. Circulation. 2003; 108:1009–14.
30. Kircher MF, Allport JR, Graves EE, Love V, Josephson L, Lichtman AH, Weissleder R. In vivo high resolution three-dimensional imaging of antigen-specific cytotoxic T-lymphocyte trafficking to tumors. Cancer Res. 2003;63:6838–46.
31. Chung TH, Wu SH, Yao M, Lu CW, Lin YS, Hung Y, Mou CY, Chen YC, Huang DM. The effect of surface charge on the uptake and biological function of mesoporous silica nanoparticles in 3T3–L1 cells and human mesenchymal stem cells. Biomaterials. 2007;28:2959–66.
32. Thorek DL, Tsourkas A. Size, charge and concentration dependent uptake of iron oxide particles by non-phagocytic cells. Biomaterials. 2008;29:3583–90.
33. Farrell E, Wielopolski P, Pavljasevic P, Kops N, Weinans H, Bernsen MR, van Osch GJ. Cell labelling with superparamagnetic iron oxide has no effect on chondrocyte behaviour. Osteoarthr Cartil. 2009;17:961–7.
34. Stoddart MJ, Grad S, Eglin D, Alini M. Cells and biomaterials in cartilage tissue engineering. Regen Med 2009;4:81–98.
35. Pawelczyk E, Arbab AS, Pandit S, Hu E, Frank JA. Expression of transferrin receptor and ferritin following ferumoxides-protamine sulfate labeling of cells: implications for cellular magnetic resonance imaging. NMR Biomed. 2006;19:581–92.
36. Aisen P, Enns C, Wessling-Resnick M. Chemistry and biology of eukaryotic iron metabolism. Int J Biochem Cell Biol. 2001;33: 940–59.